The Astronomical Journal, 139:1668–1680, 2010 April doi:10.1088/0004-6256/139/4/1668

THE MULTIPLE PRE-MAIN-SEQUENCE SYSTEM HBC 515 IN L1622

Bo Reipurth[1,2], George Herbig[3], and Colin Aspin[1]
[1] Institute for Astronomy, University of Hawaii, 640 N. Aohoku Place, Hilo, HI 96720, USA; reipurth/caa@ifa.hawaii.edu
[2] The Niels Bohr International Academy, The Niels Bohr Institute, Blegdamsvej 17, DK-2100 Copenhagen, Denmark
[3] Institute for Astronomy, University of Hawaii, 2680 Woodlawn Drive, Honolulu, HI 96822, USA; herbig@ifa.hawaii.edu
Received 2009 November 19; accepted 2010 January 13; published 2010 March 12

ABSTRACT

The bright pre-main-sequence star HBC 515 (HD 288313) located in the L1622 cometary cloud in Orion has been studied extensively with optical/infrared imaging and ultraviolet/optical/infrared spectroscopy. The spectra indicate that HBC 515 is a weakline T Tauri star (TTS) of spectral type K2V. Adaptive optics imaging in the *K* band reveals that HBC 515 is a binary with two equally bright components separated by 0.″5. A very faint third component is found 5″ to the northwest. *Spitzer* IRAC and MIPS observations show that at mid-infrared wavelengths this third source dominates the system, suggesting that it is a protostar still embedded in the nascent cloud of HBC 515. The close association of a weakline TTS with a newborn protostar in a multiple system is noteworthy. Two nearby TTSs are likely associated with the HBC 515 multiple system, and the dynamical evolution of the complex that would lead to such a configuration is considered.

Key words: accretion, accretion disks – binaries: close – stars: formation – stars: individual (HBC 515) – stars: pre-main sequence

1. INTRODUCTION

It is well established that pre-main-sequence (PMS) stars have an excess of binaries compared to the main sequence (Reipurth & Zinnecker 1993; Leinert et al. 1993; Ghez et al. 1993). Subsequent studies have confirmed and refined this result, and the separation distribution function for binaries as a function of age is gradually becoming better understood.

Knowledge about higher-order multiples is much more limited. Studies show significant incompleteness in the statistics of multiple stars even for nearby field stars (e.g., Tokovinin 2008). Various surveys have been performed in search of multiple systems among PMS stars (e.g., Duchêne et al. 2004; Ratzka et al. 2005; Correia et al. 2006). Multiple stars are particularly interesting because they most likely undergo significant dynamical evolution at early stages of their evolution. Studies of non-hierarchical multiple systems show that they are unstable and eject one or more members into either a distant orbit or a complete escape (e.g., Sterzik & Durisen 1995, 1998; Delgado-Donate et al. 2004). Such disintegration events occur in most cases during the protostellar stage, and some of the ejected objects may not have assembled enough mass to reach the hydrogen-burning stage, and so will end up as some of the many brown dwarfs found in star-forming regions (Reipurth 2000; Reipurth & Clarke 2001). This scenario has found recent support in the infrared imaging surveys of protostellar sources by Connelley et al. (2008a, 2008b, 2009), who have shown that Class I sources have a significant excess of distant companions, which gradually disappear as the cloud cores dissipate, leading to a weakened gravitational binding of these distant components.

The L1622 cloud in Orion hosts the young star HBC 515 (HD 288313), which is surrounded by a bright reflection nebula (see Figure 1). HBC 515 ($V \sim 10$) is one of the visually brightest known young low-mass stars (Herbig & Bell 1988). Luminous PMS stars are commonly found in star-forming clouds, often surrounded by bright reflection nebulae, thus lending a characteristic appearance to regions of young stars. Such bright stars generally fall into one of the two categories: either they are Herbig Ae/Be stars (Herbig 1960) or they are FU Orionis objects (Herbig 1977a). In nearby clouds, also some T Tauri stars (TTSs) illuminate bright reflection nebulae. HBC 515 is relatively unstudied, thus motivating the following in-depth analysis which among other things has revealed that it apparently forms a pentuple system.

2. OBSERVATIONS

HBC 515 was observed at the 10 m Keck I telescope with the High Resolution Echelle Spectrometer (HIRES) on three occasions, on 2002 December 16, on 2003 December 12, and on 2006 December 10. In 2002 the exposure time was 1 × 1200 s. In 2003 the exposure time was 3 × 900 s, and the seeing was about 1″. In 2006, the exposure time was 1 × 900 s, and the seeing was 1.″3. In all cases the slit was 0.″86 wide and 7″ long.

Adaptive optics *K*-band imaging of HBC 515 was performed using the 8 m Subaru telescope on 2003 December 15. The observations were done with the Infrared Camera and Spectrograph (IRCS) employing a pixel scale of 0.″0225 pixel^{-1}. Additional AO-assisted *K*-band spectroscopy was carried out using a slit with 0.″15 width.

The L1622 cloud was imaged with the 8 m Subaru telescope and SuprimeCam on 2006 January 4 through an Hα filter with a FWHM of 99 Å and a peak transmission of 87.8% at 6596 Å. The seeing was 0.″75, and five 2 minute exposures were executed plus one 20 s exposure.

The low-dispersion long-wavelength *IUE* observations of HBC 515 were carried out on 1984 March 31 under program FC232 (PI: Reipurth), with the data identifier LWP03061. HBC 515 was exposed for 3120 s.

The Infrared Telescope Facility (IRTF) was used with SpeX (Rayner et al. 2003) on 2005 January 24 to obtain a 10 minute exposure of the 0.8–2.5 μm spectral region with SXD and another 10 minute exposure of the 2.5–5.0 μm region with LXD. The spectral resolution ranges from ∼1000 to ∼2000. The data were reduced with Spextool (Vacca et al. 2003; Cushing et al. 2004).

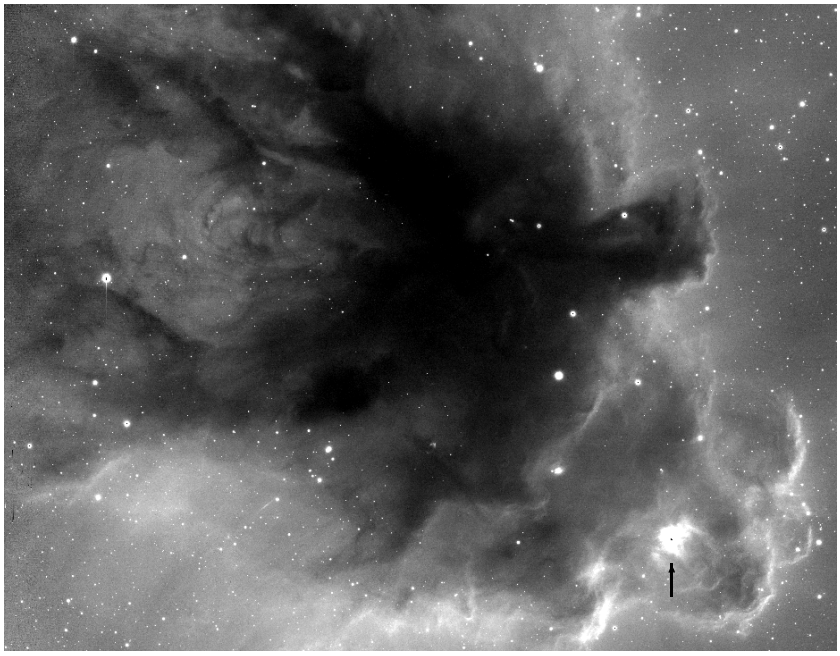

Figure 1. "Head" of the cometary L1622 cloud as seen in an Hα image obtained with the 8 m Subaru telescope. The figure is approximately $20' \times 30'$. HBC 515 is the very bright nebulous star to the southwest near the apex of the cometary cloud and is marked by an arrow. North is up and east to the left.

3. STAR FORMATION IN L1622

HBC 515 (HD 288313 = V1793 Ori = BD+1°1156 = IRAS 05513+0139) is a bright ($V \sim 9.7$, $K \sim 6.9$) young star[4] located in the L1622 cometary cloud northeast of the Orion Nebula Cluster (see Figure 1). It has spectral type K2V (Racine 1968; Herbig 1977b) and is surrounded by an extended reflection nebula called vdB62 (van den Bergh 1966) or Parsamian 3 (Parsamian 1965). Photometric observations have demonstrated that HBC 515 is a low-amplitude ($\Delta V \sim 0.1$ mag) variable with a 2.26 day period, most probably caused by cool starspots (Mekkaden et al. 2007).

The L1622 cloud contains a number of other young stars. Herbig & Rao (1972) found four bright Hα emission stars, LkHα 334–337. LkHα 336 is a multiple system with three components (Correia et al. 2006). Subsequently, Ogura & Hasegawa (1983) found several more faint Hα emission stars, including L1622-6 located about 17″ WNW of HBC 515. Several of these stars were confirmed as Hα emitters by Wiramihardja et al. (1989) and Nakano et al. (1995). *Spitzer* has identified a number of infrared excess objects in L1622, so the total young stellar population in the cloud is at least 32 (Reipurth et al. 2008). Recently, Kun et al. (2008) obtained optical spectroscopy and photometry of many of the PMS stars in L1622 and determined their physical parameters. An HH object, HH 122, has been found in the L1622 cloud (Reipurth & Madsen 1989), and more recently a number of fainter HH flows have been identified (Bally et al. 2009).

Various estimates of the distance to the L1622 cloud are found in the literature. The cloud forms part of the molecular cloud complex in Orion and Monoceros, and Maddalena et al. (1986) quote Herbst (private communication) for a distance of 500 ± 140 pc, consistent with the general distance of the Orion OB stars. However, Knude et al. (2002) studied color excesses of stars toward L1622 and found two jumps in the extinction, one at about 160 pc and another at around 400 pc, and suggest that L1622 is associated with one of them. Wilson et al. (2005) used only three stars measured by Hipparcos and located toward L1622 to suggest a very close distance of 120 pc, with 1σ errors of (+20, −8 pc). It is noteworthy that the L1622 cloud shows a pronounced cometary shape, pointing straight away from the O9.5V star σ Ori. Figure 2 shows that L1622 is located in the tenuous outer layers of Barnard's Loop. There are a number of cometary clouds surrounding σ Ori, the most famous being the Horsehead, all pointing toward the O star (see Ogura & Sugitani 1998 for a map). This is strong evidence for an association between L1622 and the σ Ori region, although the other OB stars in the Orion region are likely to contribute to its cometary appearance. σ Ori itself has a somewhat uncertain distance, Garrison (1967) and Sherry et al. (2008) advocate a distance of 440 ± 40 pc (see also Hernandez et al. 2005), whereas the Hipparcos distance from Brown et al. (1994) is 360 ± 70 pc. These measurements are all consistent with a distance of about 400 pc. The angular distance between σ Ori and HBC 515 is 5.°7, corresponding to a projected physical separation of 40 pc. The morphology of L1622 suggests that one sees the cometary cloud approximately from the side, indicating that it is not likely to be significantly closer than σ Ori. Most recently, Bally et al. (2009) have used the surface brightness of the Hα rim of L1622 to argue for a distance consistent with that of the OB stars in the Orion region. Also, Kun et al. (2008) favor a distance of 400 pc. Altogether, it appears that a reasonable distance to L1622 is 400 pc, which is adopted in the following.

L1622 has been observed in a number of millimeter-wavelength transitions (e.g., Maddalena et al. 1986; Wilson et al. 2005), and in these studies it is usually named Orion-East, a name that originated with Herbig & Rao (1972). The center of the cloud has been shown to consist of two condensations in N_2H^+, which form a filament oriented along the axis of the cometary cloud (Lee et al. 2001). L1622 has also attracted attention since it was detected in the centimeter-wave continuum (Casassus et al. 2006), offering evidence for very small grains, or electric dipole radiation from hydrogenated fullerenes (Iglesias-Groth 2006).

[4] Equatorial coordinates $\alpha = 05{:}54{:}03.0$, $\delta = +01{:}40{:}22$ (J2000); Galactic coordinates $l = 204.77$, $b = -11.95$.

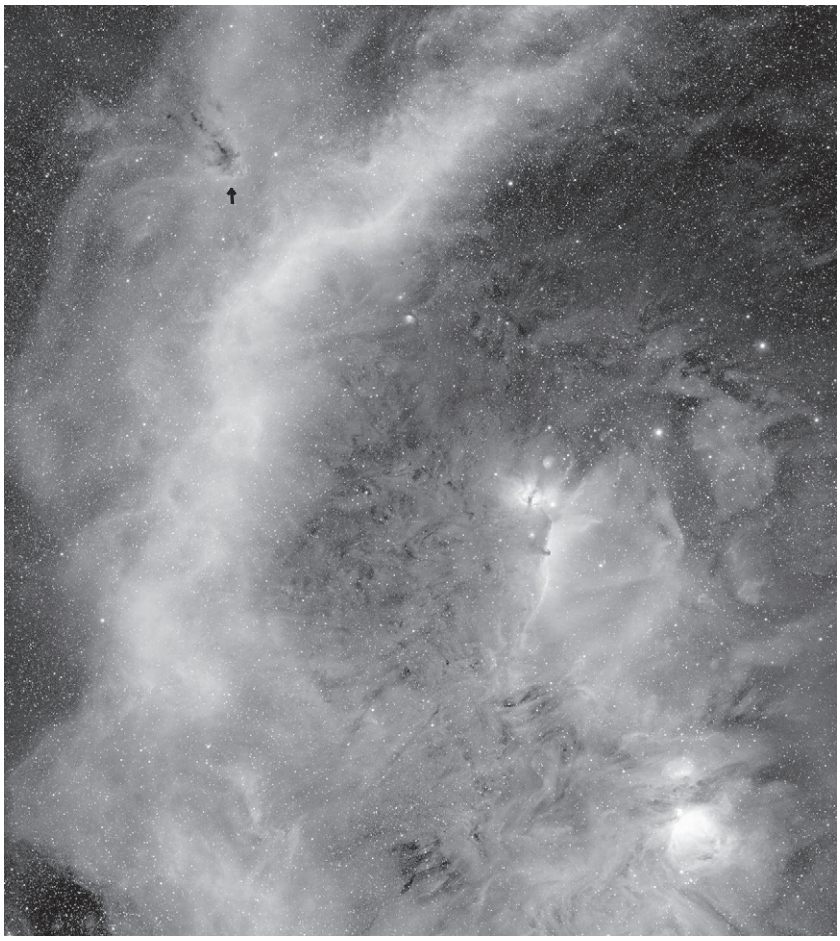

Figure 2. Wide-field Hα image of the region around L1622. Barnard's Loop is toward the upper left, and L1622 is located to the northeast in the outskirts of the Loop, marked by an arrow. L1622 is pointing straight toward σ Ori, as is the Horsehead, and several other cometary clouds in the region. The figure is approximately $9^\circ \times 10^\circ$. North is up and east is left. Image courtesy Drew Sullivan.

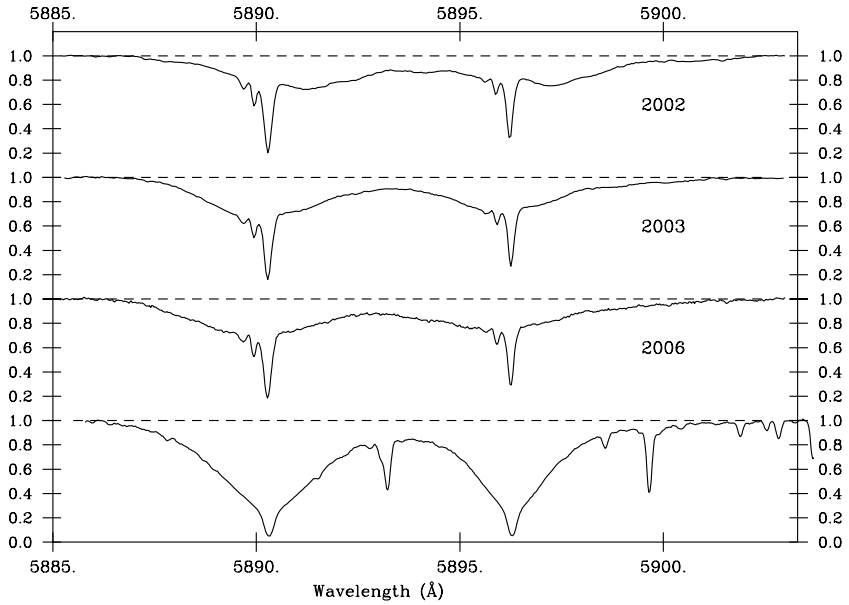

Figure 3. Keck HIRES spectra of the Na I lines in HBC 515 at three epochs. The spectrum of HD 219134, a K3 V star, is shown at the bottom for reference.

4. RESULTS

4.1. High Dispersion Optical Spectra

HBC 515 was observed with HIRES in 2002, 2003, and 2006 (see Section 2 for details). Figures 3, 5, 6, and 7 show selected regions of the spectrum, compared to the same regions of the spectrum of HD 219134, a reference star of spectral type K3 V. No strong emission lines are found in the spectral range observed. The most prominent feature in the absorption spectrum is the Na I doublet at 5890/5896 Å. Figure 3 shows

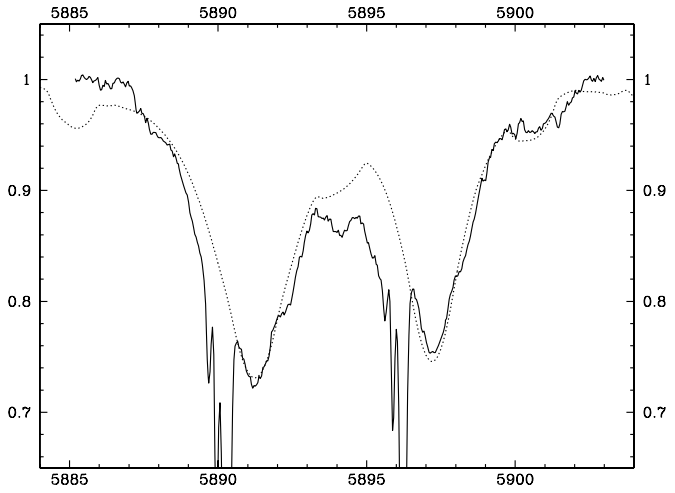

Figure 4. Observed spectrum of HBC 515 in 2002 (solid) and the representation of the same structure created by the procedure described in the text (dotted): a K3 V dwarf spun up to $v \sin i = 40$ km s^{-1}, shifted to $v_\odot = +65$ km s^{-1} and weighted by 0.35, plus a flat continuum weighted by 0.65. The narrow features extending off the bottom of the figure are interstellar and are not included in this simulation.

that region for the three epochs. The major absorption features are the narrow interstellar $D_{2,1}$ (5890, 5896 Å) lines at +16.8 ± 0.3 km s^{-1} (equivalent widths [W] = 184, 121 mÅ), which lie within the broad stellar Na I lines.[5] Two weaker narrow features are also present, at −14.0 ± 0.1 (W = 15 and 7 mÅ) and at −0.8 ± 0.2 km s^{-1} (W = 29 and 20 mÅ). Both the velocities and the intensities remain almost constant over the period of observation, and are very probably interstellar.

These interstellar Na I lines are projected upon a very wide absorption trough, which on the shortward side stretches to at least −165 km s^{-1}. On the longward side, the wing is equally pronounced, although the edge is more difficult to define, but it seems to extend to at least the same (positive) velocity. It should be noted that the pressure broadened wings of the Na I lines in the K3 V reference star extend to approximately the same velocities (see the bottom panel of Figure 3).

The general features of the extended Na I structure in 2002 can be reproduced as the sum of a flat continuum that contributes about 0.65 of the total flux in this region, and a K3 V spun up to about $v \sin i = 40$ km s^{-1} and shifted to about $v_\odot = +65$ km s^{-1}; it provides the remaining 0.35. Figure 4 shows the resulting "composite" spectrum (dotted) superposed upon the observed one.

The 2003 spectrum can be similarly fitted, but with 0.48 of the total contributed by the K star and 0.52 by the continuum, the former shifted to $v_\odot = +10$ km s^{-1}. In 2006, the proportions were the same but the K star shift was to +5 km s^{-1}. (These velocities are estimated to be uncertain by several km s^{-1}.) They are repeated in the last line of Table 1, where it is seen that in 2002 they coincide with feature *c*, and in 2003 and 2006 approximately, where a blend of *a* and *b* would be expected. The features *a*, *b*, and *c* are discussed further below and are interpreted in more detail in Section 5.

The very prominent Hα absorption line is shown in Figure 5. It is rather shallow, with varying equivalent width, presumably a consequence of the structural changes seen between epochs in narrower metallic lines, described below. A central emission peak is present in Hα at about +16 km s^{-1}—near the stellar velocity—at all three epochs. Also apparent in Figure 5 are weak, narrow emissions at [N II] 6548 and 6583. On these spectrograms, the sky background obtained in windows 1″–2″ wide on either side of the star's spectrum has been subtracted, and the velocities and equivalent widths of the stellars [N II] and [O I] 6300, 6363, and [S II] 6716, 6730 are given in Table 2. The same features are present also in the sky background. The mean velocity of all the measurable [N II] and [S II] lines in HBC 515 is +15 ± 1 km s^{-1}, and +17 ± 1 km s^{-1} in the background; the difference is not significant. Not surprisingly, these are very near the velocity of the background molecular cloud and that of HBC 515 itself. The forbidden lines (Table 2) clearly do not share what is possibly the orbital motion of the sources responsible for the above-mentioned absorption-line structure, which varies from one epoch to another.

Li I λ6707 is quite strong in HBC 515. Figure 6 shows the region around this lithium line and the neighboring Ca I λ6717 line. The equivalent width of the λ6707 line ranges from 0.42 Å (2002) to 0.36 Å (2003) to 0.41 Å (2006), but the differences are near the uncertainties in the location of the continuum level. The measures of W(6707) by Mekkaden et al. (2007), at a resolution of R ∼2400, range between 0.37 Å and 0.58 Å (typical error 0.05 Å) over an interval of 1.2 years, with no dependence on the photometric period of 2.26 days. Small variations in λ6707 equivalent widths have also been observed in some young stars (Patterer et al. 1993) related to magnetic activity and star spots. Also, Stout-Batalha et al. (2000) noted that the Li I 6707 line in RW Aurigae is enhanced when accretion rates increase. Figure 6 shows major structural changes from epoch to epoch in the lithium line. Additionally, these changes are mirrored in the adjacent Ca I λ6717 line. The structure of the lithium and calcium lines is generally not seen in the numerous other absorption lines in the spectrum of HBC 515, except for certain Fe I lines. Figure 7 shows a region between 5440 Å and 5480 Å, where three Fe I lines are present. All of these lines mimic the structure seen in the Hα line as well as in the Li I and Ca I lines (see Table 1). In 2002, three features (labeled *a*, *b*, and *c* in Table 1) were clearly identified, with $v_\odot$ of approximately −95, −8, and +66 km s^{-1}. In 2003, only two features were visible, with $v_\odot$ of about −20 and +38 km s^{-1}. The variability of this structure is discussed in Section 5.

4.2. Ultraviolet Spectra

A low-dispersion ultraviolet spectrum of HBC 515 in the range from 2400 Å to 3350 Å has been obtained with the *IUE* satellite. The spectrum is shown in Figure 8, where the version included in the homogeneously reduced atlas of *IUE* spectra of PMS stars by Valenti et al. (2003) has been chosen. HBC 515 shows a well-defined continuum with weak emission from the unresolved Mg II 2800 line. The Mg II line is a resonance doublet (λλ2795.53 and 2802.71 Å) and is the strongest near-ultraviolet feature seen in the spectra of TTSs, and has been extensively studied both theoretically and observationally (e.g., Ardila et al. 2002). The Mg II line flux in HBC 515 is 1.8 × 10^{-13} erg s^{-1} cm^{-2}.

4.3. AO K-band Imaging

HBC 515 was observed with adaptive optics in the *K* band at the Subaru 8 m telescope, and the resulting image is shown in

[5] Unless otherwise noted, all velocities are in the heliocentric system. The rest velocity of HBC 515 is expected to be near +18 km s^{-1}, which is the average of the radio-frequency measurements of the velocity of the L1622 cloud (Brooks et al. 1976; Ho et al. 1978; Maddalena et al. 1986; Lee et al. 2001; Kun et al. 2008).

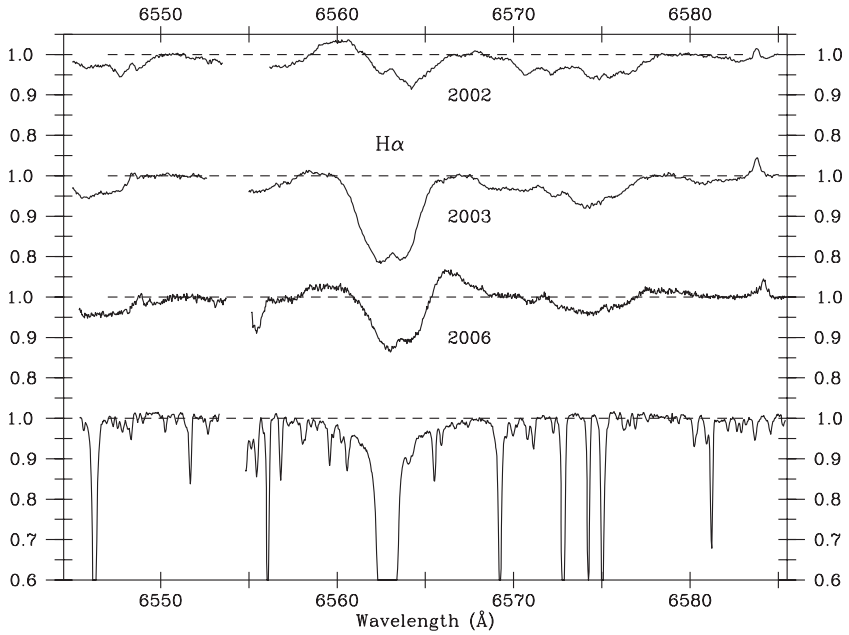

Figure 5. Keck HIRES spectra of the Hα line in HBC 515 at three epochs. An instrumental artifact has been removed around 6554 A. Weak emission is seen at [N II] 6548 and [N II] 6584 and is possibly from the surrounding H II region. The spectrum of HD 219134, a K3 V star, is shown at the bottom for reference.

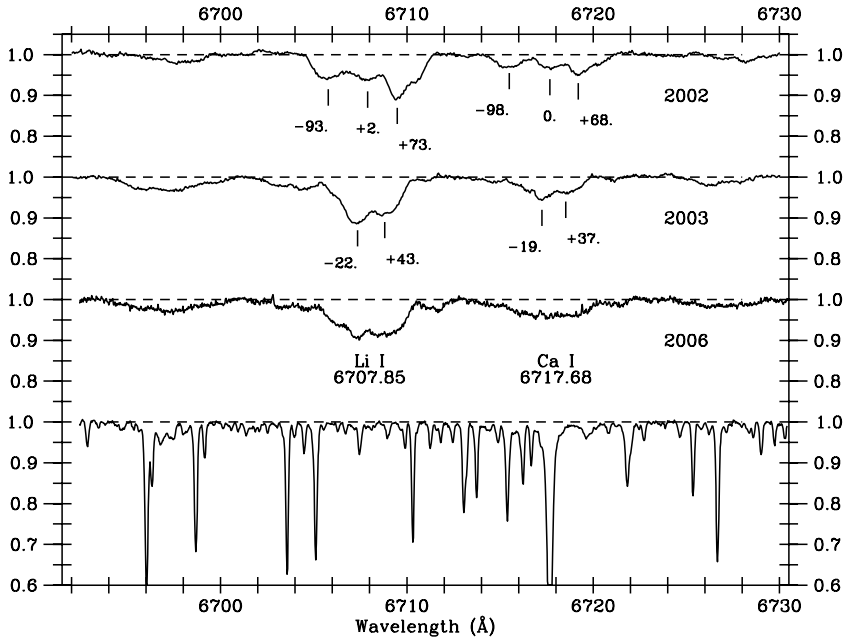

Figure 6. Keck HIRES spectra of the lithium and calcium lines in HBC 515 at three epochs. The spectrum of HD 219134, a K3 V star, is shown at the bottom for reference.

Figure 9. The observations reveal that HBC 515 is a close binary with components of almost identical brightness. Henceforth the bright optical component is referred to as HBC 515A, and the individual components as Aa and Ab. Component Aa to the east is marginally brighter than component Ab, with a flux ratio of 1.03. The separation of the components is about 0.″5, and the position angle of component Ab relative to Aa is 259°. The point-spread function of component Ab is slightly elongated along the axis of the system, with a FWHM of 0.″123 compared to a FWHM of 0.092 for the Aa component. This might possibly indicate that Ab itself could also be a binary, however the observations were performed under difficult seeing conditions, so further observations are required to establish whether the Ab component is a binary.

4.4. Infrared Spectroscopy

A near-infrared spectrum covering the range from 1 to 4 μm was obtained of HBC 515 using SpeX at the IRTF. Part of the spectrum in the 1.0–1.3 μm region is seen in Figure 10. The spectrum shows a wealth of absorption lines, with no features in emission. We are indebted to Michael Connelley for running his code that matches equivalent widths of photospheric absorption lines with those from spectral standards in the SpeX library (Rayner et al. 2009).[6] Based on equivalent widths of 44 lines, the numerical goodness of fit is strongly peaked at a spectral type of K2, with acceptable fits in the range K0–K5. The code

[6] The SpeX spectral library is available at http://irtfweb.ifa.hawaii.edu/~spex/IRTF_Spectral_Library/.

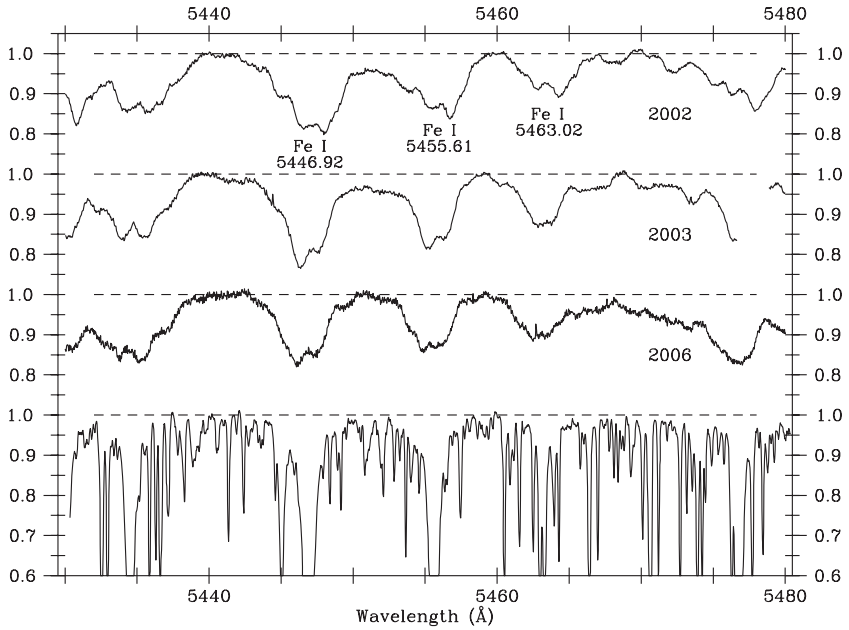

Figure 7. Keck HIRES spectra of three Fe I lines (5447, 5455, 5463) in HBC 515 at three epochs. Note that an instrumental artifact has been removed around 5478 A in the 2003 spectrum. The spectrum of HD 219134, a K3 V star, is shown at the bottom for reference.

Table 1
Heliocentric Velocities of Absorption Line Components in HBC 515

Line	Wavelength	2002			2003		2006	
		a	*b*	*c*	*a*	*b*	*a*	*b*
Fe I (15)	5446.917	−97	−15:	+60	−30	+33	−40	+23
Fe I (15)	5455.610	−92	−1	+64	−19	+39	−39	+17:
Fe I (1163)[a]	5463.02	···	−17	+68	−15	···	−33	···
Na I	5889.953	···	···	+66	···	···	···	···
Na I	5895.923	···	···	+67	···	···	···	···
Hα	6562.817	···	−14	+63	−14	+38	−8	+36
Li I	6707.85	−93	0	+73	−22	+43	−38	+25:
Ca I	6717.685	−98	0	+68	−19	+37	···	···
Mean		−95	−8	+66	−20	+38	−32	+27
Composite		···	···	+65	+10		+5	

Note. [a] Blend of two lines at 5463.276 and 5462.959 Å.

Table 2
Heliocentric Velocities and Equivalent Widths of Narrow Emission Lines in HBC 515

Line	Wavelength	$v_\odot$ (km s^{-1})			W (mÅ)[a]		
		2002	2003	2006	2002	2003	2006
[O I]	6300.304	+12.	···	+15.	8.	···	6.
[O I]	6363.776	···	···	+16.	···	···	2.
[N II]	6548.05	+16.	+19.	+18.	5.	6.	10.
Hα	6562.817	+10.	+15.	+22.:	···	···	···
[N II]	6583.45	+15.	+18.	+14.	7.	24.	23.
[S II]	6716.47	···	+13.	+13.	···	2.:	2.:
[S II]	6730.87	+14.	+14.	+14.	8.	6.	7.

Note. [a] Note that these Ws are measured with respect to the immediately adjacent structure, not to the overall continuum level.

allows veiling as a free parameter, but no veiling was required to obtain a consistent fit with the spectral standards. The most prominent features in the near-infrared spectrum of HBC 515 are the CO bands in the 2.3–2.4 μm region. The equivalent width of the first CO band is 6.58 ± 0.52 Å, and the value for a

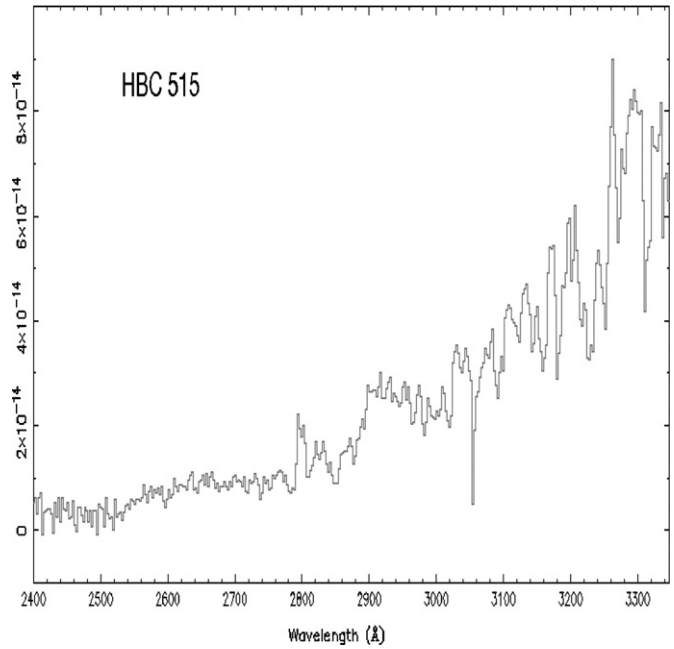

Figure 8. Ultraviolet *IUE* spectrum of HBC 515 between 2400 and 3347 A. The flux scale is in erg cm^{-2} s^{-1} A^{-1}.

K2V standard is 6.52 ± 0.46 Å. So, the infrared spectral type of HBC 515 is in perfect agreement with the optical classification of K2V obtained by Racine (1968) and Herbig (1977b). An unusual spectral feature in the near-infrared spectrum of HBC 515 is a strong high-excitation He I absorption line at 1.083 μm (see Figure 10). We discuss the presence of this line in Section 5.

Given that HBC 515 has been resolved into two components, it is of interest to learn if the infrared spectrum is due to both components or is dominated by one of them. While obtaining adaptive optics imaging of HBC 515 we also acquired adaptive optics low-resolution *K*-band spectroscopy of the individual components. The resulting spectra are shown in Figure 11. The

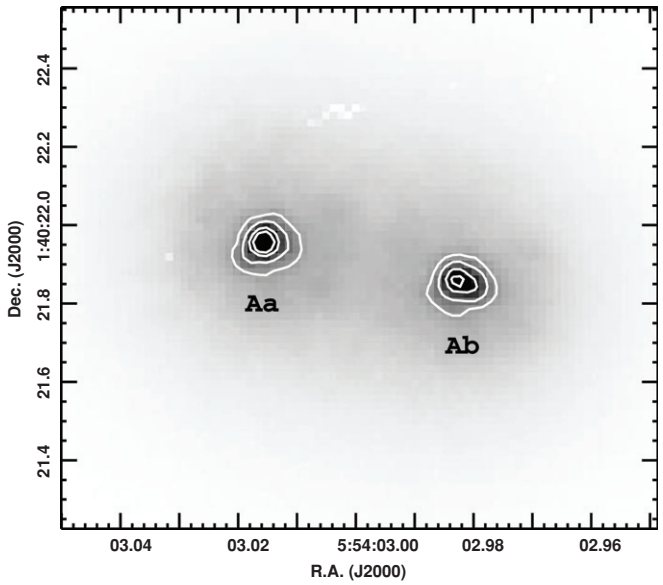

Figure 9. *K*-band image of HBC 515 with adaptive optics obtained at the Subaru telescope. The observations reveal HBC 515 to be a 0.″5 binary, with component Aa marginally brighter than component Ab. North is up and east is left.

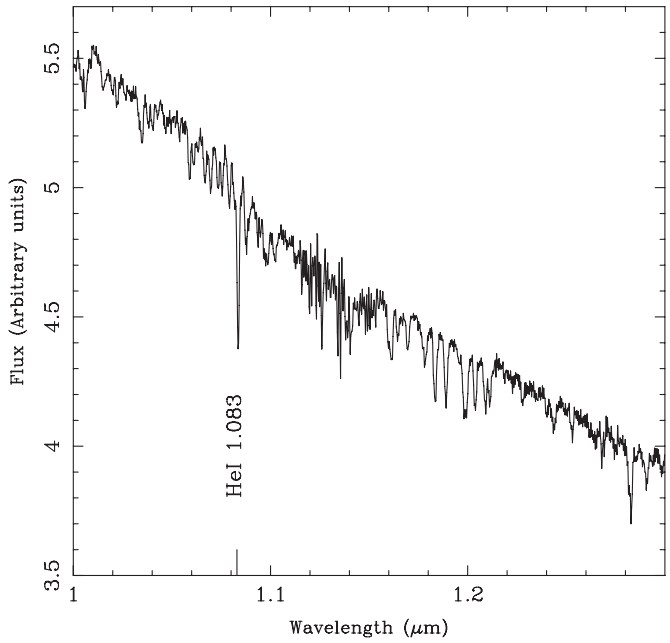

Figure 10. Near-infrared region from 1.0 to 1.3 μm in HBC 515. The figure is a section of a 1–4 μm spectrum obtained with SpeX at the IRTF. The well-defined photospheric lines allow for an accurate spectral classification. The He I line at 1.083 μm is highly unusual for the spectral type. The higher noise in the continuum around 1.13 μm is due to terrestrial effects.

CO bands are a little stronger in the western slightly fainter component (Ab), suggesting that it may have a marginally later spectral type, but the two components are evidently very similar.

4.5. Spitzer Mid-Infrared Imaging

In the AO *K*-band image of HBC 515 one sees a faint star, here called HBC 515B, at a separation of 5.″3 from HBC 515A and at a position angle of 41° (see Figure 12). *Spitzer* archival images from IRAC and MIPS were used to derive the 3.6, 4.5, 5.8, and 8 μm magnitudes given in Table 3. Figure 13 is a mosaic of those IRAC images. In all four images, four sources are visible,

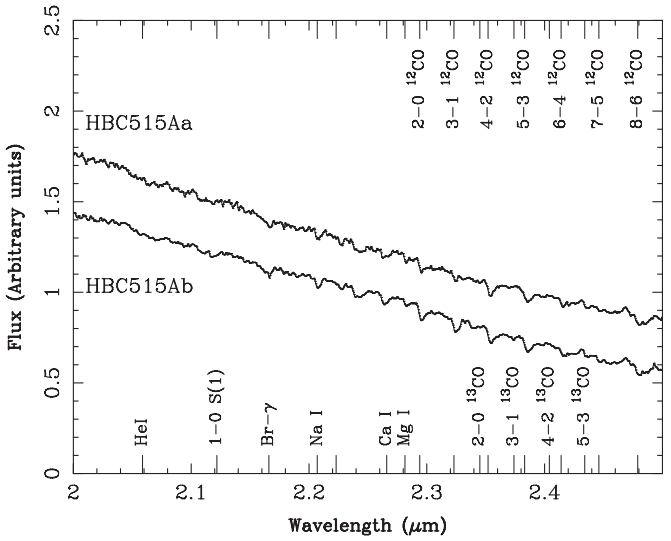

Figure 11. Low-resolution *K*-band spectra of the HBC 515 A components obtained with adaptive optics at the Subaru telescope. The spectra have virtually the same flux levels and are here displaced from each other for clarity.

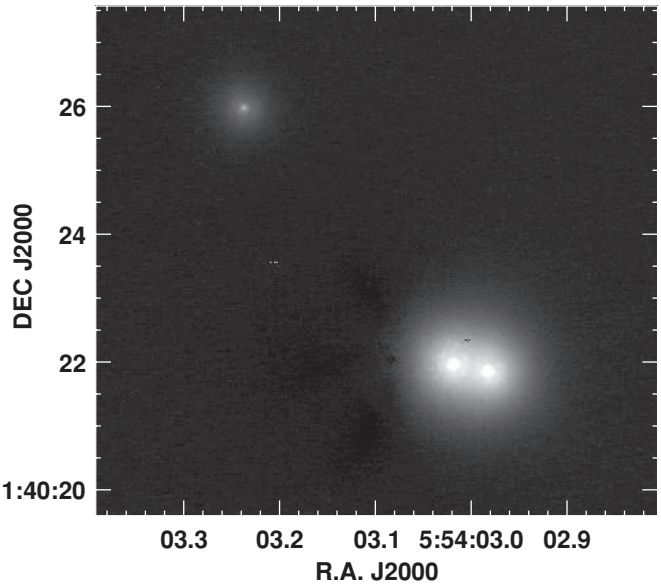

Figure 12. *K*-band image with adaptive optics of the close HBC 515A binary (bottom right) and its faint companion HBC 515B (top left) at a separation of 5.″3.

and at the shortest wavelengths HBC 515A is the brightest, but the B-component is much brighter than in the *K* band. At 5.8 μm, B is as bright as A, and at 8 μm it is the dominant source in the system. Figure 14 shows the MIPS 24 μm image; at this wavelength, the B-component completely overwhelms the much fainter A-component.

The other two sources visible in the *Spitzer* images are L1622-6 about 17″ to the west, and a faint source about 36″ NNW of HBC 515, which Kun et al. (2008) have dubbed L1622-6N and found to be an Hα emission star. Figure 15 shows the location of these objects in a near-infrared color–color diagram. It appears that the fourth star is an infrared-excess object, and thus part of a little grouping of young stars surrounding HBC 515. L1622-6 and L1622-6N are likely to be physically associated with HBC 515; in the following they are designated as HBC 515C and HBC 515D, respectively.

Table 3
The Components of the HBC 515 System

	A	B	C	D
Alt. ID	HBC 515		L1622-6	L1622-6N
α_{2000}	5:54:03.0	5:54:03.2	5:54:01.9	5:54:02.0
δ_{2000}	+01:40:22	+01:40:26	+01:40:27	+01:40:56
V[a]	10.01 ± 0.02	···	15.86 ± 0.02	18.42 ± 0.06
R[a]	9.26 ± 0.02	···	14.46 ± 0.02	16.87 ± 0.04
I[a]	8.83 ± 0.02	···	12.64 ± 0.02	14.88 ± 0.03
J[b]	7.69 ± 0.02	···	10.62 ± 0.03	12.57 ± 0.02
H[b]	7.13 ± 0.04	···	9.90 ± 0.03	11.84 ± 0.02
K[b]	6.94 ± 0.03	10.36 ± 0.05[e]	9.58 ± 0.02	11.36 ± 0.02
3.6[c]	6.95 ± 0.04	8.01 ± 0.05	9.28 ± 0.01	10.66 ± 0.01
4.5[c]	6.83 ± 0.07	7.46 ± 0.05	9.12 ± 0.01	10.32 ± 0.01
5.8[c]	6.90 ± 0.07	6.70 ± 0.06	9.01 ± 0.01	9.97 ± 0.01
8.0[c]	6.82 ± 0.03	6.22 ± 0.04	8.43 ± 0.01	9.25 ± 0.01
24[d]	···	2.41 ± 0.01	3.77 ± 0.02	6.57 ± 0.02

Notes.
[a] From Kun et al. (2008).
[b] 2MASS.
[c] *Spitzer* IRAC (photometry for A and B uncertain because of their proximity).
[d] *Spitzer* MIPS.
[e] From AO image, using 2MASS value for HBC 515.

4.6. Photometry of HBC 515

Table 3 lists the available optical and infrared photometry of HBC 515 and its components, obtained from Kun et al. (2008) and from the Two Micron All Sky Survey (2MASS) and *Spitzer* data sets. Additionally, *IRAS* detected HBC 515 at 12, 25, and 60 μm, with flux densities of 0.52, 1.16, and 11.37 Jy. The uncertainty ellipse has a semimajor axis and a semiminor axis of 19″ and 6″, respectively, at a position angle of 88°. This means that the observed fluxes combine contributions from HBC 515A, B, and C. This has been partitioned by adding the *Spitzer* 24 μm fluxes for components B and C, and subtracting this from the *IRAS* 25 μm flux to arrive at the contribution for HBC 515A. In view of the energy distributions of components A and C, the entire 60 μm flux has been attributed to HBC 515B. The resulting energy distributions are shown in Figure 16.

Spectral energy distributions for a large range of stellar and disk parameters have been calculated by Robitaille et al. (2006, 2007), and the data points shown in Figure 16 have been compared to their models. The constraints posed by the photometry have narrowed the relevant models from Robitaille et al., and the four panels in Figure 17 show the possible remaining fits to the four components of HBC 515. Conclusions about the individual stars are drawn below.

HBC 515A. The spectral energy distribution of this close K2V binary is very well matched by a blackbody with a temperature of about 5000 K and a modest extinction of $A_V \sim 1$. Only at the very longest wavelength at which photometry is available, 24 μm, there is a clear deviation from a blackbody, indicating the presence of circumstellar material (Figures 16–18). The lack of observations at longer wavelengths, however, makes it impossible to constrain the properties of this disk material. Integration under the 5000 K blackbody yields a luminosity of 23 $L_\odot$. If the components are identical, each has a luminosity of ∼11.5 $L_\odot$. If this is compared to the PMS evolutionary tracks of D'Antona & Mazzitelli (1994), a formal fit suggests that each component of the binary is a 1.8 $M_\odot$ star with an age of only about 500,000 years. The narrow spacing of the Hayashi evolutionary tracks as a function of effective temperature means that the individual masses could be anywhere in the 1.5–2.0 $M_\odot$ range. The stars are close to the end of their Hayashi tracks, and will next turn onto their radiative tracks where they will rapidly appear as late Herbig Ae stars, ultimately reaching the main sequence as A stars (see Gray & Corbally 1994 for a relation between effective temperature and spectral type).

HBC 515B. As noted earlier, the B-component is heavily extincted, is invisible at optical wavelengths, but emerges in

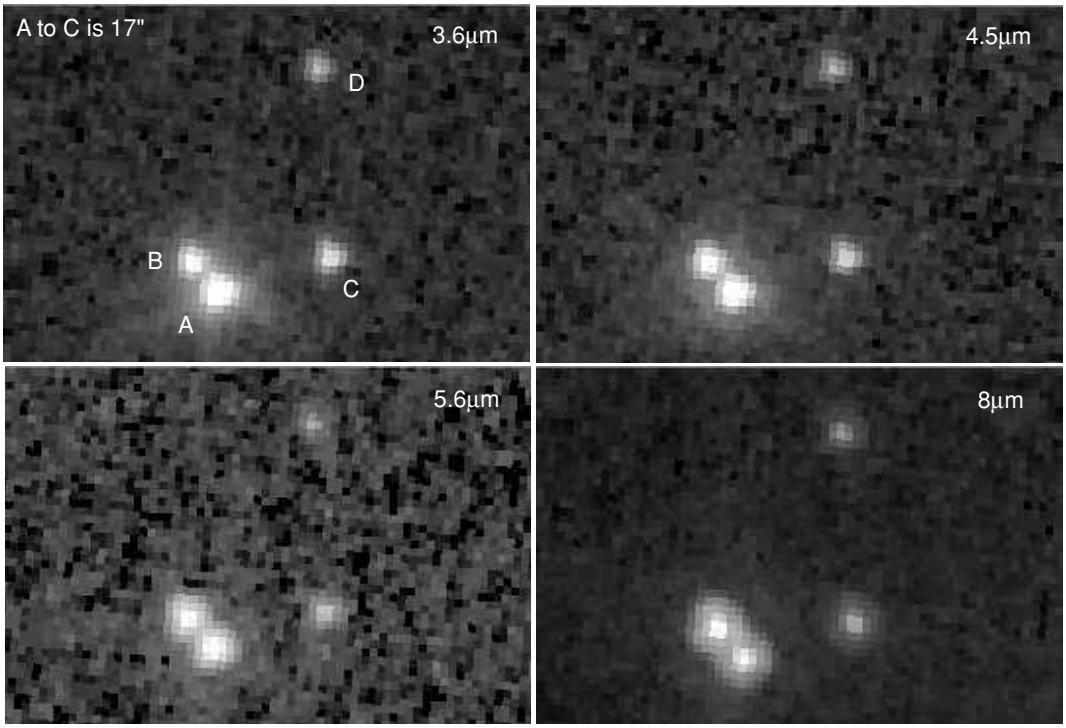

Figure 13. Small clustering surrounding HBC 515 as seen with *Spitzer* at 3.6, 4.5, 5.8, and 8 μm. HBC 515A is the southernmost of the four stars. Each panel is approximately 50″ × 80″. North is up and east is left.

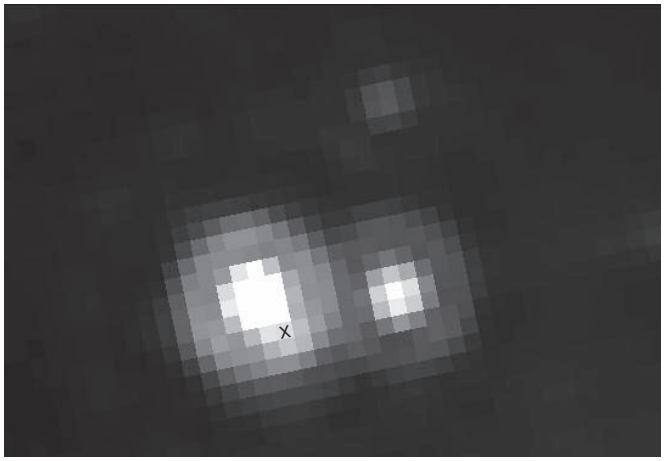

Figure 14. Small clustering surrounding HBC 515 as seen with *Spitzer* at 24 μm. HBC 515A is marked with a cross. HBC 515B completely dominates the pair at mid-infrared wavelengths. The panel is approximately 50″ × 80″, and north is up and east is left.

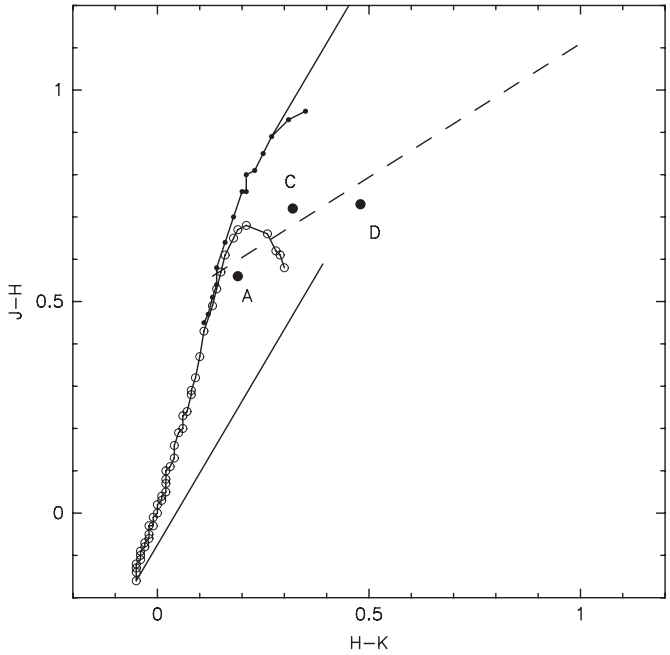

Figure 15. J–H vs. H–K diagram showing three of the components of the HBC 515 multiple system. A is HBC 515, C is L1622-6, and D is L1622-6N. Reddening vectors corresponding to $A_V = 6$ magnitudes are shown extending from the extremes of the main sequence and giant branch (solid lines). The dash-dotted line is the locus of classical TTSs.

the *K* band, and rapidly brightens toward longer wavelengths, and completely dominates all the other components at 24 μm. The *Spitzer* color–color diagram in Figure 18 suggests that the object is at the border between the Class I and Class II sources. The energy distribution indicates the presence of substantial circumstellar material. The total luminosity in the observable range from 2.2 μm to 60 μm is 1.6 $L_\odot$. This is certainly seriously affected by extinction. If we, merely as a matter of exercise, assume that HBC 515B is similar to (one of) the components in HBC 515A, then we can crudely connect a 5000 K blackbody curve to the shortest wavelength data points if an extinction A_V of about 20 mag is applied.

HBC 515C. This object has a spectral type of M4 based on optical spectroscopy by Kun et al. (2008) and it shows Hα in emission. The spectral energy distribution of HBC 515C out to 8 μm shows only a minor deviation from a stellar blackbody (Figure 17), indicating that only a small amount of warm circumstellar material in an inner disk is present. But the surprisingly large 24 μm flux shows that a much larger reservoir of cool circumstellar material is present at larger distances. This is the spectral behavior of the rare class of transitional disks, which are interpreted as having an optically thin inner disk surrounded by an optically thick outer disk, or possessing an inner gap in the disk, possibly due to planet formation (e.g., Najita et al. 2007). The characteristic energy distribution of the HBC 515C star is reminiscent of the transitional disks around GM Aur and DM Tau (e.g., Calvet et al. 2005). The luminosity of HBC 515C in the observed range from 0.5 to 24 μm is 1.3 $L_\odot$.

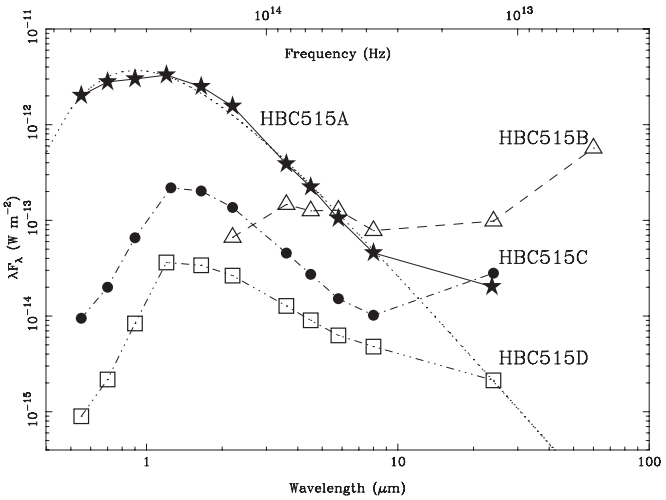

Figure 16. Energy distributions of the components of the HBC 515 multiple system. A Planck curve for a 5000 K black body with $A_V = 1$ has been fitted to the observed data for HBC 515A.

HBC 515D. The spectral energy distribution of HBC 515D is very typical of TTSs and indicates the presence of a circumstellar disk. The spectral type of the star is M3 according to Kun et al. (2008), and it shows Hα emission. The MIPS observation at 24 μm is not sufficient to constrain the cool outer disk material. The luminosity of HBC 515D from 0.5 to 24 μm is 0.3 $L_\odot$.

4.7. ROSAT X-ray Detection of HBC 515

The *ROSAT* all-sky survey bright source catalog (Voges et al. 1999) contains a quite bright X-ray source, 1RXS J055402.6+014024, which coincides with the position of HBC 515. The count rate is 0.26 ± 0.02 count s^{-1}, and the hardness ratios 1 and 2 are 0.97 ± 0.02 and 0.30 ± 0.08, respectively, among the most common for *ROSAT* sources. While the astrometric accuracy of the *ROSAT* sources is very good, the very large beam of *ROSAT* means that components A, B, C, and D are all included, and examination of the point-spread function shows that the profile is elongated toward C and D, and in fact is brightest on the western side, suggesting that these two sources contribute significantly to the detection. Little can be said other than that the X-ray detection of the HBC 515 system is unsurprising for a group of young stars.

4.8. The Reflection Nebula of HBC 515

HBC 515 is surrounded by a large reflection nebula known as vdB 62 (van den Bergh 1966) or Parsamian 3 (Parsamian 1965). Figure 19 shows a contour plot of the nebula, which stretches

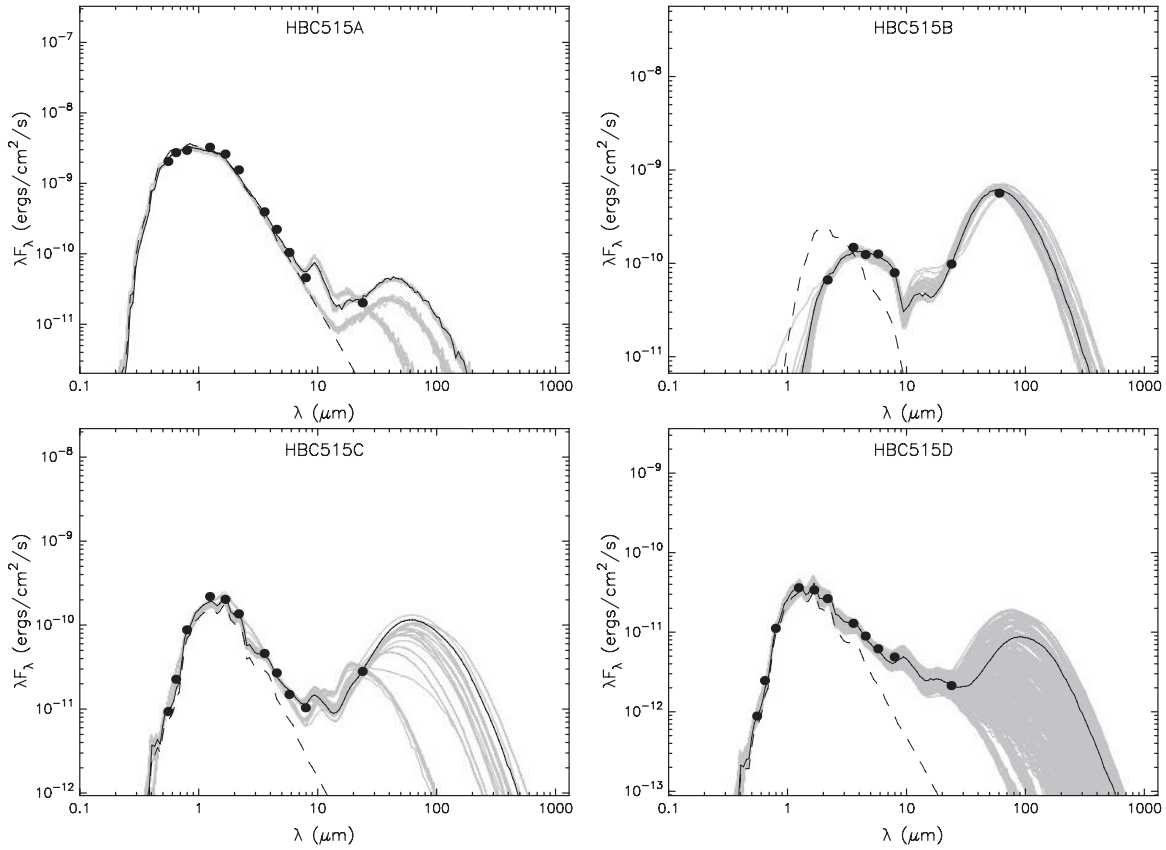

Figure 17. Energy distributions of the four components of the HBC 515 system with fits to the large database of disk and envelope models of Robitaille et al. (2006); see the text for details.

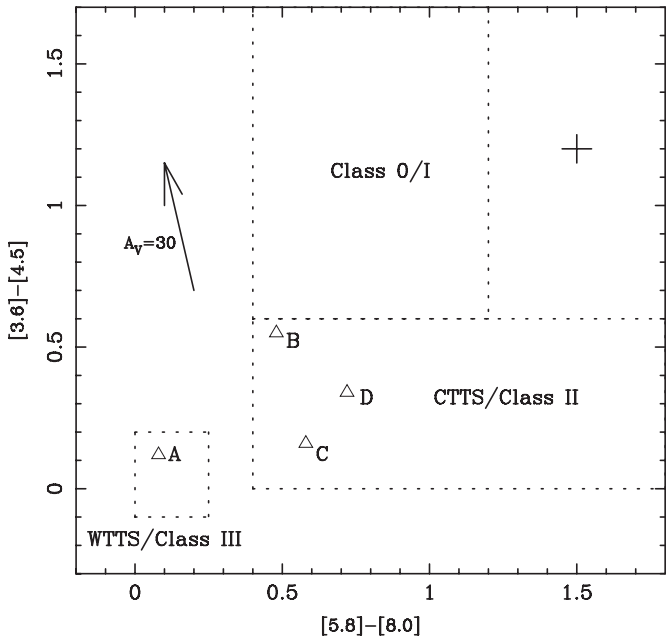

Figure 18. Position of HBC 515 A, B, C, and D in an IRAC color–color diagram. The boxes indicate the general locations of Class 0/I/II/III objects from Allen et al. (2004). The cross in the upper right corner gives an estimate of the uncertainties of the individual points.

over almost 1′. The morphology of the inner region, with its one-armed spiral structure, is reminiscent of the reflection nebulae around several FUors (e.g., Goodrich 1987). Examination of the inner contours suggests that either HBC 515 is seen down through a cavity that is approximately directed toward the observer or HBC 515 is located above the cloud surface and illuminates it. Either case would explain why the star is not heavily extincted.

4.9. Other Binaries and Multiples in L1622

The two lists of PMS stars in L1622 by Kun et al. (2008) and Reipurth et al. (2008) contain a total of 32 young stars and embedded sources. Some of these are in binary systems, specifically the binary L1622-10 and the triple system LkHα 336 (Reipurth & Zinnecker 1993). The deep Hα image taken at the Subaru 8 m telescope in 0.″75 seeing has been searched for new visual binaries. Eight of the embedded sources have no optical counterpart and three objects are outside the field of the CCD image. Among the remainder, one more binary system is discovered, it is detected in the 2MASS survey as 2MASS05540455+0142587 and is located roughly 3′ north of HBC 515 (see Figure 20). The binary has a separation of about 1.″6 with the fainter companion at position angle 105° and is associated with a compact reflection nebula extending toward the southwest (Figure 21). The primary is visibly elongated, and since the point-spread function of the image is perfectly circular, this suggests that either the primary is an unresolved binary itself or the star is associated with a compact reflection nebula.

5. DISCUSSION

In the following, various issues that have been motivated by the observations described in the previous sections are considered.

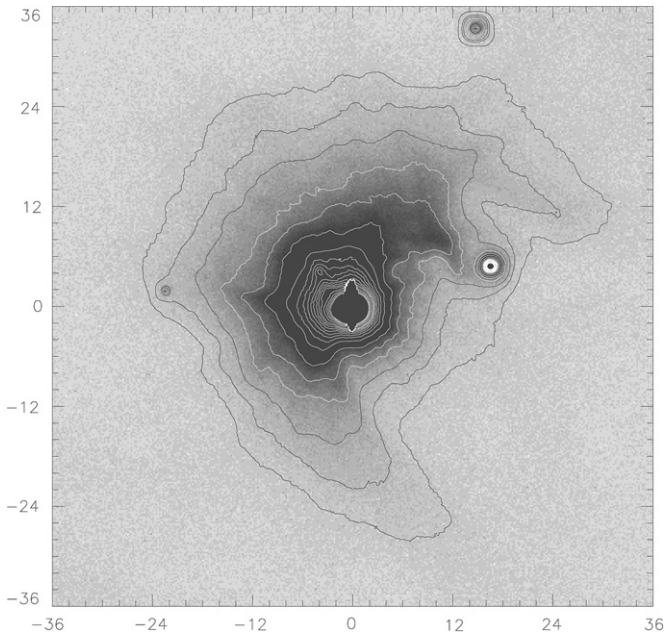

Figure 19. Direct image showing the surroundings of HBC 515 taken with an Hα narrowband filter. HBC 515 suffers a bit of charge overflow due to saturation. The seeing during the 20 s exposure was 0.″7. The contours represent the logarithm of the counts, with values of (from the outermost inward) 3.9984 (smoothing factor 12), 3.999 and 4.000 (smoothing 9), 4.002, 4.005, 4.01, 4.02 (smoothing 3) and 4.03–4.20 with steps of 0.01 and no smoothing. Tickmarks are in arcseconds. The deeply embedded infrared companion HBC 515B is very weakly visible about 5″ to the NE, and the two low-luminosity companions HBC 515C and D are seen 17″ to the west and 36″ to the NNW, respectively.

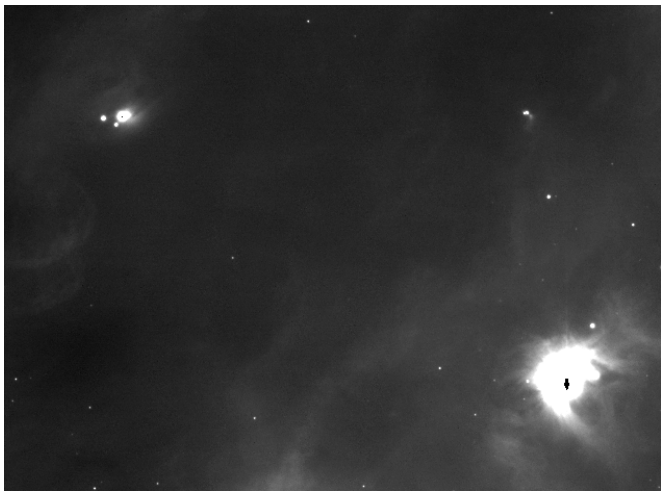

Figure 20. Region around HBC 515 (in the lower right corner) harbors two other systems, the LkHα 336 non-hierarchical triple system (in the upper left corner) and the new close binary 2MASS05540455+0142587 (upper right corner). The image is taken with the Subaru 8 m telescope through an Hα filter and the field is approximately 4′ × 5.′5, with north up and east left.

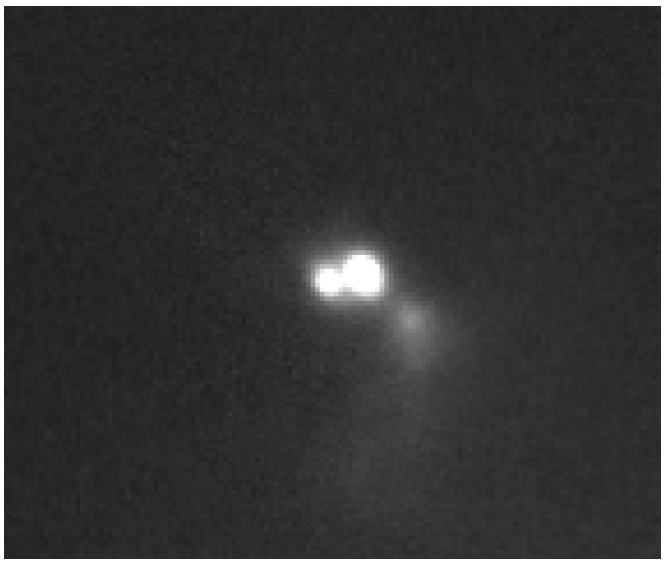

Figure 21. Enlargement from the previous figure showing the new close binary 2MASS05540455+0142587. The elongation of the primary is evident. The field is approximately 15″ wide, with north up and east left.

Understanding the Structure of Lithium in HBC 515. In Section 4.1, it was noted that considerable structure is seen in Li I 6707 and Ca I 6717, in Hα, and in several Fe I lines. This structure is reproduced in all of these lines, but varies from epoch to epoch. Table 1 gives the velocities measured for the various components seen at each epoch. It is evident that there are three well-defined features in the 2002 spectrum and two features in the 2003 and 2006 spectra, which within each epoch and within the errors of measurement are consistent for the various transitions listed.

Such structure seems to indicate the presence of three stellar components in the HBC 515 binary, which implies that at least one of the components detected with AO must be a spectroscopic binary. This is not at all an unreasonable assumption, as is discussed below. However, it should be noted that the multiple structures are *not* seen in any other of the hundreds of well-defined photospheric lines in the rich spectrum of HBC 515. The complex structures are visible only at Hα, and in the lines of Li I 6707, Ca I 6717, and in certain Fe I lines, and their motion is consistent with the shifts in the Na I doublet (Section 4.1). These lines have in common that they all have a very low-excitation potential. The behavior of the lithium line is particularly interesting. Herbig (2008) found that Li I 6707 could change into emission in the EXor V1118 Ori, and in a detailed study of the classical FUor V1057 Cyg, Herbig (2009) found that Li I 6707 showed several components changing with time, which were ascribed to variations in the powerful winds from the FUor. Hence, an alternative interpretation of the multiple structures is that a similar phenomenon is seen in HBC 515. Finally, if at least one of the two HBC 515A components is a close binary, then the orbital motion may stir up the circumstellar material remaining in the system, leading to broad, multiple, high-velocity structures detectable in absorption in low-excitation lines. If there is only little such material close to the star, this would be consistent with the absence of infrared excess in HBC 515. The present observations do not permit one to choose between these three interpretations.

The He I 1.083 Absorption Line in HBC 515. An unusual feature of the near-IR spectrum of HBC 515 is a strong ($W = 1.7 \pm 0.2$ Å) *absorption* line near the position of the first member of the 2^3S–n^3P^o series of He I at 1.08303 μm. He I lines are found in *emission* in both the optical and the near-IR region of TTSs (Beristain et al. 2001; Takami et al. 2002). P Cygni structure at 1.083 μm in some active TTS has been discussed by Edwards et al. (2003, 2006). In such objects energetic infall phenomena and hot inner disk winds are believed to be responsible: since the lower state of 1.083 μm is metastable, 19.7 eV above the ground, it must be fed by decay of higher He I levels populated by some high-temperature process.

1.083 μm and the next member of that series at 3888 Å have been found in absorption against the continua of OB stars in the Orion Nebula and M8 (Wilson 1940; Münch & Wilson 1962; Oudmaijer et al. 1997). In that environment, the over-population of 2^3S is not so surprising, although the precise mechanism is unclear; one possible explanation is absorption by inhomogeneities in the surrounding H II region. But 1.083 μm absorption has also been found in cooler stars, first shown in a study by Zirin (1982), and later in a survey of K–M stars by Lambert (1987). It has also been reported in H-deficient carbon stars by Geballe et al. (2009) and in a metal-deficient red giant by Dupree et al. (1992).

Clearly there is ample precedence for the appearance of 1.083 μm in absorption in a star as cool as HBC 515. It should be noted, however, that there may be a contribution from Si I 1.0827 μm: see the high-resolution spectra of similarly cool stars published by Lambert (1987).

The Mid-Infrared Companion. The nature of the infrared companion revealed by *Spitzer* is not well constrained by the available observations. From its energy distribution and the fact that it is heavily extincted, it is either a deeply embedded TTS or a protostar, presumably a Class I source. The existence of a deeply embedded protostar next to a visible young star is not unique, other cases include V1735 Cyg SM1 located about 20″ northeast of the FUor V1735 Cyg (Sandell & Weintraub 2001), Re 13 SM located about 7″ from Re 13 (Sandell & Weintraub 2001), as well as deeply embedded mid-infrared or submillimeter sources next to the Herbig Ae/Be stars LkHα 198 (Sandell & Weintraub 1994), LkHα 234 (Weintraub et al. 1994; Cabrit et al. 1997), and LkHα 225S (Looney et al. 2006). It appears, however, that the close association of a weakline TTS and a deeply embedded young star in a multiple system is highly unusual.

HBC 515A: Proto-Algols or a Quadruple System? In Section 4.6, a comparison of the observed parameters for HBC 515A with theoretical evolutionary tracks suggested that the two very similar components would soon evolve into Herbig Ae/Be stars. However, instead of explaining the considerable brightness of HBC 515A as due to components of fairly high mass, another possibility is that HBC 515A is not only a binary, but also a quadruple system containing four T Tauri-like stars. Adaptive optics observations with even higher resolution than the present ones would be needed to test this alternative hypothesis. It is of interest, however, to consider the evolution of such a quadruple system. Reipurth & Aspin (2004) suggested that quadruple systems that have recently transformed from a non-hierarchical to a hierarchical configuration would be progenitors of the rare visual binaries in which each component is a FUor. If HBC 515A is indeed a quadruple system, then the close quadruple encounter required for such a transformation would severely truncate the circumstellar material of the components, and might be the cause of their current appearance as weakline TTSs. However, the small remaining and truncated circumstellar disks are fed from a circumbinary disk through gas streams, and this as well as other dynamical effects causes each close binary orbit to shrink (Artymowicz & Lubow 1996). Eventually the components in each of the two close binaries get so close that their remaining disks interact, and each pair erupts in FUor outbursts, producing a wide binary system with two FUors. If this alternative interpretation of HBC 515A is correct, then the HBC 515 system may still have surprises in store.

The Distant Components in the HBC 515 Multiple System. As noted earlier, HBC 515 is associated with two nearby young stars, one 17″ and another 36″ distant, which are here denoted as HBC 515C and D, respectively. Given the low space density of known young stars in the L1622 cloud, it appears highly unlikely that these two stars are unrelated to the star formation activity that produced the HBC 515 system. Rather, they could well be dynamically ejected into extended bound orbits around the principal HBC 515A/B system. Once the compact cloud core associated with HBC 515A/B is dispersed, these outliers are likely to gently drift away (Connelley et al. 2008a, 2008b, 2009).

In conclusion, the seemingly disparate observational facts about HBC 515 discussed in this paper appear to be best understood in terms of the dynamical evolution of the components in a newborn multiple system.

Michael Connelley is thanked for preparing the contour plot of the nebula around HBC 515 and for running his spectral classification code on the infrared SpeX spectra, Thomas Robitaille for his advice on his models, and Drew Sullivan for the use of Figure 2. B.R. is thankful for hospitality at the Niels Bohr International Academy, Copenhagen, where part of this paper was written. This work is based in part on data collected at the Subaru Telescope, which is operated by the National Astronomical Observatory of Japan (NAOJ). Some of the data presented herein were obtained at the W.M. Keck Observatory from telescope time allocated by the University of Hawaii Time Allocation Committee. The Observatory was made possible by the generous financial support of the W.M. Keck Foundation. This project was supported by the Gemini Observatory, which is operated by the Association of Universities for Research in Astronomy, Inc., on behalf of the international Gemini partnership of Argentina, Australia, Brazil, Canada, Chile, the UK, and the US. This work is based in part on observations made with the *Spitzer Space Telescope*, which is operated by the Jet Propulsion Laboratory, California Institute of Technology under a contract with NASA. This research has made use of the SIMBAD database, operated at CDS, Strasbourg, France, and of NASA's Astrophysics Data System Bibliographic Services. B.R. acknowledges support by the National Science Foundation under grant NSF AST-0407005. This material is based upon work supported by the National Aeronautics and Space Administration through the NASA Astrobiology Institute under cooperative agreement no. NNA08DA77A issued through the Office of Space Science.

REFERENCES

Allen, L. E., et al. 2004, ApJS, 154, 363
Ardila, D. R., Basri, G., Walter, F. M., Valenti, J. A., & Johns-Krull, C. M. 2002, ApJ, 567, 1013
Artymowicz, P., & Lubow, S. H. 1996, ApJ, 467, L77
Bally, J., Walawender, J., Reipurth, B., & Megeath, S. T. 2009, AJ, 137, 3843
Beristain, G., Edwards, S., & Kwan, J. 2001, ApJ, 551, 1037
Brooks, J. W., Sinclair, M. W., Manefield, G. A., & Goss, W. M. 1976, MNRAS, 177, 299
Brown, A. G. A., de Geus, E. J., & de Zeeuw, P. T. 1994, A&A, 289, 101
Cabrit, S., Lagage, P.-O., McCaughrean, M., & Olofsson, G. 1997, A&A, 321, 523
Calvet, N., et al. 2005, ApJ, 630, L185
Casassus, S., Cabrera, G. F., Förster, F., Pearson, T. J., Readhead, A. C. S., & Dickinson, C. 2006, ApJ, 639, 951
Connelley, M., Reipurth, B., & Tokunaga, A. 2008a, AJ, 135, 2496
Connelley, M., Reipurth, B., & Tokunaga, A. 2008b, AJ, 135, 2526
Connelley, M. S., Reipurth, B., & Tokunaga, A. T. 2009, AJ, 138, 1193
Correia, S., Zinnecker, H., Ratzka, Th., & Sterzik, M. F. 2006, A&A, 459, 909
Cushing, M. C., Vacca, W. D., & Rayner, J. T. 2004, PASP, 116, 362
D'Antona, F., & Mazzitelli, I. 1994, ApJS, 90, 467

Delgado-Donate, E. J., Clarke, C. J., Bate, M. R., & Hodgkin, S. T. 2004, MNRAS, 351, 617
Duchêne, G., Bouvier, J., Bontemps, S., André, P., & Motte, F. 2004, A&A, 427, 651
Dupree, A. K., Sasselov, D. D., & Lester, J. B. 1992, ApJ, 387, L85
Edwards, S., Fischer, W., Hillenbrand, L., & Kwan, J. 2006, ApJ, 646, 319
Edwards, S., Fischer, W., Kwan, J., Hillenbrand, L., & Dupree, A. K. 2003, ApJ, 599, L41
Garrison, R. F. 1967, PASP, 79, 433
Geballe, T. R., Kameswara Rao, N., & Clayton, G. C. 2009, ApJ, 698, 735
Ghez, A., Neugebauer, G., & Matthews, K. 1993, AJ, 106, 2005
Goodrich, R. W. 1987, PASP, 99, 116
Gray, R. O., & Corbally, C. J. 1994, AJ, 107, 742
Herbig, G. H. 1960, ApJS, 4, 337
Herbig, G. H. 1977a, ApJ, 217, 693
Herbig, G. H. 1977b, ApJ, 214, 747
Herbig, G. H. 2008, AJ, 135, 637
Herbig, G. H. 2009, AJ, 138, 448
Herbig, G. H., & Bell, K. R. 1988, Lick Obs. Bull. No., 1111
Herbig, G. H., & Rao, N. K. 1972, ApJ, 174, 401
Hernandez, J., Calvet, N., Hartmann, L., Briceno, C., Sicilia-Aguilar, A., & Berlind, P. 2005, AJ, 129, 856
Ho, P. T. P., Barrett, A. H., & Martin, R. N. 1978, ApJ, 221, L117
Iglesias-Groth, S. 2006, MNRAS, 368, 1925
Knude, J., Fabricius, C., Høg, E., & Makarov, V. 2002, A&A, 392, 1069
Kun, M., Balog, Z., Mizuno, N., Kawamura, A., Gáspár, A., Kenyon, S. J., & Fukui, Y. 2008, MNRAS, 391, 84
Lambert, D. L. 1987, ApJS, 65, 255
Lee, C. W., Myers, P. C., & Tafalla, M. 2001, ApJS, 136, 703
Leinert, Ch., et al. 1993, A&A, 278, 129
Looney, L. W., Wang, S., Hamidouche, M., Safier, P. N., & Klein, R. 2006, ApJ, 642, 330
Maddalena, R. J., Morris, M., Moscowitz, J., & Thaddeus, P. 1986, ApJ, 303, 375
Mekkaden, M. V., Muneer, S., & Raveendran, A. V. 2007, MNRAS, 378, 1079
Münch, G., & Wilson, O. C. 1962, Z. Astrophys., 56, 127
Najita, J. R., Strom, S. E., & Muzerolle, J. 2007, MNRAS, 378, 369
Nakano, M., Wiramihardja, S. D., & Kogure, T. 1995, PASJ, 47, 889
Ogura, K., & Hasegawa, T. 1983, PASJ, 35, 299
Ogura, K., & Sugitani, K. 1998, PASA, 15, 91
Oudmaijer, R. D., Drew, J. E., Barlow, M. J., Crawford, I. A., & Proga, D. 1997, MNRAS, 291, 110
Parsamian, E. S. 1965, Izv. Akad. Nauk Armyan. SSR Ser. Fiz.-Math, 18, 146
Patterer, R. J., Ramsey, L., Huenemoerder, D. P., & Welty, A. D. 1993, AJ, 105, 1519
Racine, R. 1968, AJ, 73, 233
Ratzka, T., Köhler, R., & Leinert, Ch. 2005, A&A, 437, 611
Rayner, J. T., Cushing, M. C., & Vacca, W. D. 2009, ApJS, 185, 289
Rayner, J. T., Toomey, D. W., Onaka, P. M., Denault, A. J., Stahlberger, W. E., Vacca, W. D., Cushing, M. C., & Wang, S. 2003, PASP, 115, 362
Reipurth, B. 2000, AJ, 120, 3177
Reipurth, B., & Aspin, C. 2004, ApJ, 608, L65
Reipurth, B., & Clarke, 2001, AJ, 122, 432
Reipurth, B., & Madsen, C. 1989, ESO Messenger, 55, 32
Reipurth, B., Megeath, S. T., Bally, J., & Walawender, J. 2008, in Handbook of Star Forming Regions, Vol. I, ed. B. Reipurth (San Francisco, CA: ASP), 782
Reipurth, B., & Zinnecker, H. 1993, A&A, 278, 81
Robitaille, T. P., Whitney, B. A., Indebetouw, R., & Wood, K. 2007, ApJS, 169, 328
Robitaille, T. P., Whitney, B. A., Indebetouw, R., Wood, K., & Denzmore, P. 2006, ApJS, 167, 256
Sandell, G., & Weintraub, D. A. 1994, A&A, 292, L1
Sandell, G., & Weintraub, D. A. 2001, ApJS, 134, 115
Sherry, W. H., Walter, F. M., Wolk, S. J., & Adams, N. R. 2008, AJ, 135, 1616
Sterzik, M., & Durisen, R. H. 1995, A&A, 304, L9
Sterzik, M., & Durisen, R. H. 1998, A&A, 339, 95
Stout-Batalha, N. M., Batalha, C. C., & Basri, G. S. 2000, ApJ, 532, 474
Takami, M., Chrysostomou, A., Bailey, J., Gledhill, T. M., Tamura, M., & Terada, H. 2002, ApJ, 568, L53
Tokovinin, A. 2008, MNRAS, 389, 925
Vacca, W. D., Cushing, M. C., & Rayner, J. T. 2003, PASP, 115, 389
Valenti, J. A., Fallon, A. A., & Johns-Krull, C. M. 2003, ApJS, 147, 305
van den Bergh, S. 1966, AJ, 71, 990
Voges, W., et al. 1999, A&A, 349, 389
Weintraub, D. A., Kastner, J. H., & Mahesh, A. 1994, ApJ, 420, L87
Wilson, O. C. 1940, ApJ, 91, 360
Wilson, B. A., Dame, T. M., Masheder, M. R. W., & Thaddeus, P. 2005, A&A, 430, 523
Wiramihardja, S. D., Kogure, T., Yoshida, S., Ogura, K., & Nakano, M. 1989, PASJ, 41, 155
Zirin, H. 1982, ApJ, 260, 655